MAGNETOHYDRODYNAMICS Vol. 51 (2015), No. 3, pp. 567–578

NUMERICAL SIMULATION OF ELECTROMAGNETIC LEVITATION IN A COLD CRUCIBLE FURNACE

S. Spitans[1,2], *E. Baake*[1], *A. Jakovičs*[2], *H. Franz*[3]

[1] *Institute of Electrotechnology, Leibniz University of Hannover, Wilhelm-Busch-Str. 4, 30167 Hannover, Germany*
[2] *Laboratory for Mathematical Modelling of Environmental and Technological Processes, University of Latvia, 8 Zellu str., LV-1002 Riga, Latvia*
[3] *ALD Vacuum Technologies GmbH, Wilhelm-Rohn Str. 35, 63450 Hanau, Germany*

Guidelines for a cold crucible (CC) levitation melting furnace design have been examined in the literature and combined for a pilot CC concept. Meanwhile, by means of external coupling between electromagnetic and hydrodynamic problems a numerical model for liquid metal flow with free surface dynamics in an alternating EM field has been developed and verified. A 3D model with Large Eddy Simulation (LES) turbulence description is applied for a case of 1 kg of liquid titanium levitation in the CC furnace at two different AC frequencies. Calculation results are compared to a simplified model of the furnace section with the k-ω SST turbulence approximation.

Introduction. The conventional induction furnace with a cold crucible (CC) is a very useful technology for electromagnetic (EM) processing of high purity materials. The application areas range from manufacturing of titanium parts for aerospace, automotive or medical industry, photovoltaic silicon purification and crystallization up to treating of nuclear fusion products [1].

Due to the air gaps, the sectioned metallic crucible is partially transparent for an EM field and acts as a secondary inductor. In this case, EM pressure prominently squeezes the melt and a semi-levitation is achieved. The crucible is cooled by water and the melt is mainly abutted upon the skull – in such a way the contamination of the melt by the crucible material is reduced. However, thermal losses through the water-cooled crucible and melt contact regions appear to be a limiting factor for reaching a higher level of overheating and efficiency.

From this point of view, the CC is an attractive option for complete EM levitation melting. In this case, there is no contact between the melt and the crucible, so the heat losses are limited only to radiation and evaporation. This ensures a higher level of superheat, permits investigation of materials at extreme temperatures and metal evaporation for coating purposes [2].

However, a complete levitation melting in the CC, the same as conventional levitation in vertical axisymmetric fields, is a challenge, because Lorentz forces vanish on the symmetry axis [3]. The melt can be kept from leakage at this lowest point on the axis of a levitated sample mainly by surface tension and thus the charge weight is limited.

At the same time, industrial requirements must be satisfied for the scale-up potential of the CC levitation melting technology and, for this purpose, accurate numerical simulation is an advantageous tool. Therefore, a numerical model for the liquid metal flow with free surface dynamics in an alternating EM field has been developed by means of external coupling between EM force recalculation in $ANSYS$, Volume of Fluid (VOF) simulation of a two-phase turbulent flow in $FLUENT$, free surface shape reconstruction in $CFD-Post$ and a self-written surface filtering procedure. Detailed verification has already approved the accuracy of our calculation approach [4]–[6].

In this work, a review of recent developments and design considerations in the field of CC construction is presented. The generalized CC design is used to simulate the levitation of 1 kg of liquid titanium by means of a full 3D model with LES turbulence description. Calculation results are compared to the simplified k-ω SST model of a single CC section.

1. Literature review and CC design considerations. In the following articles [7], [8], it is shown that levitation in the CC with a small number of segments can lead to a flower-like charge shape and undesirable contact between the molten metal and the centre of a palisade. Furthermore, a cone-shaped CC is considered to be the best for a stable levitation melting [7]–[9]. Application of different AC frequencies f for lower and upper inductors can be tailored specially for separate control of levitation (with several kHz) and heating (with several tens of kHz) [7], [9]. Taking into account these considerations, authors were able to levitate and melt 2.3 kg of titanium in two to three minutes [7].

In [2], it is stressed that on a larger scale the mechanism of levitation confinement is considerably differently from a small droplet case, where surface tension plays the key role. The numerical investigation has led to a conclusion that the levitation of a large fluid mass requires a high AC frequency, because a lower penetration depth concentrates the EM force near the free surface and stabilizes it. On top of that, the higher intensity of a turbulent flow that perturbs free surface corresponds to a lower AC frequency and a greater penetration depth. Full levitation of 2 kg of titanium melt was achieved in a 2D k-ω numerical simulation using an EM field frequency of 20 kHz. Despite the lack of EM forces and insufficient surface tension forces on the axis of the melt, the leakage was not observed in the simulation. A specific tangential flow along the surface away from the bottom stagnation point ensured dynamic confinement of the levitated melt.

The work [8] describes the design, optimization and experimental realization of a CC levitation melting system for light alloys. With the appropriate shape of the lower part of the CC it was possible to compress the magnetic field lines through the nozzle at the bottom of the crucible and to increase the field gradient around the critical null point. Moreover, stability of the levitated melt was enhanced by the null-field region introduced by a number of reverse turns. As a result, few hundred grams of the light metal alloy were successfully melted and solidified under the levitation conditions using the 1 kHz frequency.

Taking into account some of these considerations, authors were able to melt 0.85 kg of titanium and 0.15 kg of tantalum under the levitation conditions and produce 1 kg of uniform composite using 3 kHz and 50 kHz for the levitation and heating coils, accordingly [9].

Numerical simulation tools have been applied to optimize the efficiency of the CC furnace [1]. The idea was to change the cross-section of a crucible segment in a way that reduces main Joule losses in the palisade along the air gap.

According to particular knowledge obtained from the literature, we have designed a prototype CC furnace for our numerical investigation of 1 kg titanium levitation melting.

2. Verification of the numerical model. In order to supplement the previous verification of our calculation approach, the classical experiment on levitation melting of a small aluminum sample ($m = 20$ g) [10] was repeated in our laboratory and simulated with 2D-axisymmetric and full 3D VOF models that utilize the k-ω SST and LES turbulence formulations. Governing equations and numerical implementation have been described previously [4].

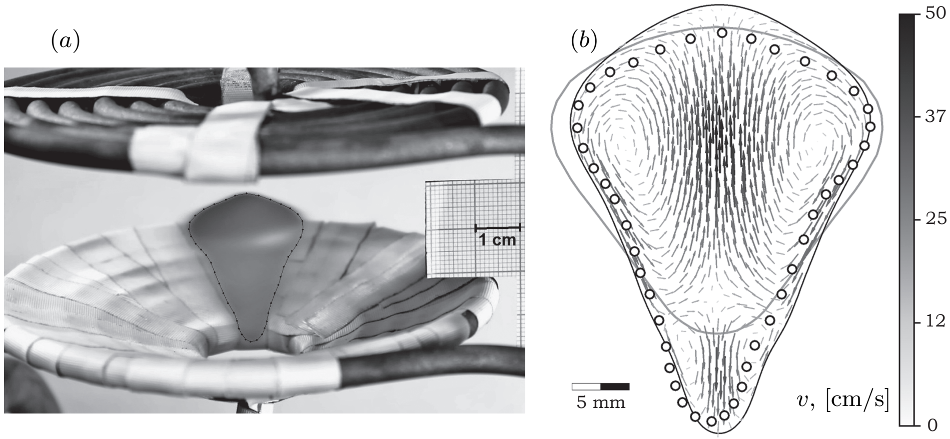

Fig. 1. Time-averaged shape of the levitated molten aluminum in experiment (*a*) and measured time-averaged free surface shape (circles), 2D k-ω SST (grey line) and 3D LES (black line and velocity) time-averaged solution (*b*).

At an initial time moment, the melt is given a spherical shape and zero velocity. Transient simulation of the free surface flow with regular Lorentz force recalculation upon the deformed shape of a droplet is performed until the fully developed flow regime is achieved.

According to our transient 2D k-ω SST calculation, the EM field, free surface shape and the flow adjust themselves to a completely steady state regime with a characteristic two-vortex structure and a maximum velocity of 25 cm/s. Meanwhile, these results differ from our measurements of the time-averaged droplet shape (Fig. 1*a*) and do not predict either the fluctuating behavior of the free surface observed in experiment under fully developed flow conditions.

The time-averaged free surface shape obtained by a 3D LES calculation (Fig. 1*b*) appears to be in a better agreement with the time-averaged measurements, and the maximum velocity of the time-averaged simulated flow proves to be twice greater than in the 2D k-ω SST calculation.

In comparison with the Reynolds-averaged flow and a smooth free surface shape obtained by the transient 2D k-ω SST calculation, the finer flow structures resolved with LES reach up to 100 cm/s and with account of dynamic pressure contribute to the free surface continuous fluctuations. Oscillations of the melt free surface shape observed in the experiment under a fully developed flow regime (Fig. 2, left column) appear to be in a good qualitative agreement with the transient 3D LES calculation results (Fig. 2, right column).

Further details on this study can be found in [11].

Particular numerical models with k-ω SST and LES turbulence description are applied for the simulation of liquid titanium levitation in a pilot-designed CC furnace.

3. Numerical models and CC geometry. Two numerical models were used for the simulation of 1 kg of liquid titanium levitation in a prototype setup: a simplified model considering a single CC section (Fig. 3*a*) and a full 3D model of the CC furnace and a titanium charge (Fig. 3*b*). An example of the numerical mesh applied for a simplified (10^5 elem.) and a full ($5{\cdot}10^5$ elem.) EM problem with fine resolution of the magnetic field penetration depth ($\delta_{\mathrm{EM}} = 2.1$ mm at 100 kHz) is shown next to the numerical mesh for the simplified ($0.8{\cdot}10^5$ elem.) and full ($13{\cdot}10^5$ elem.) transient hydrodynamic (HD) calculation of the two-phase turbulent flow.

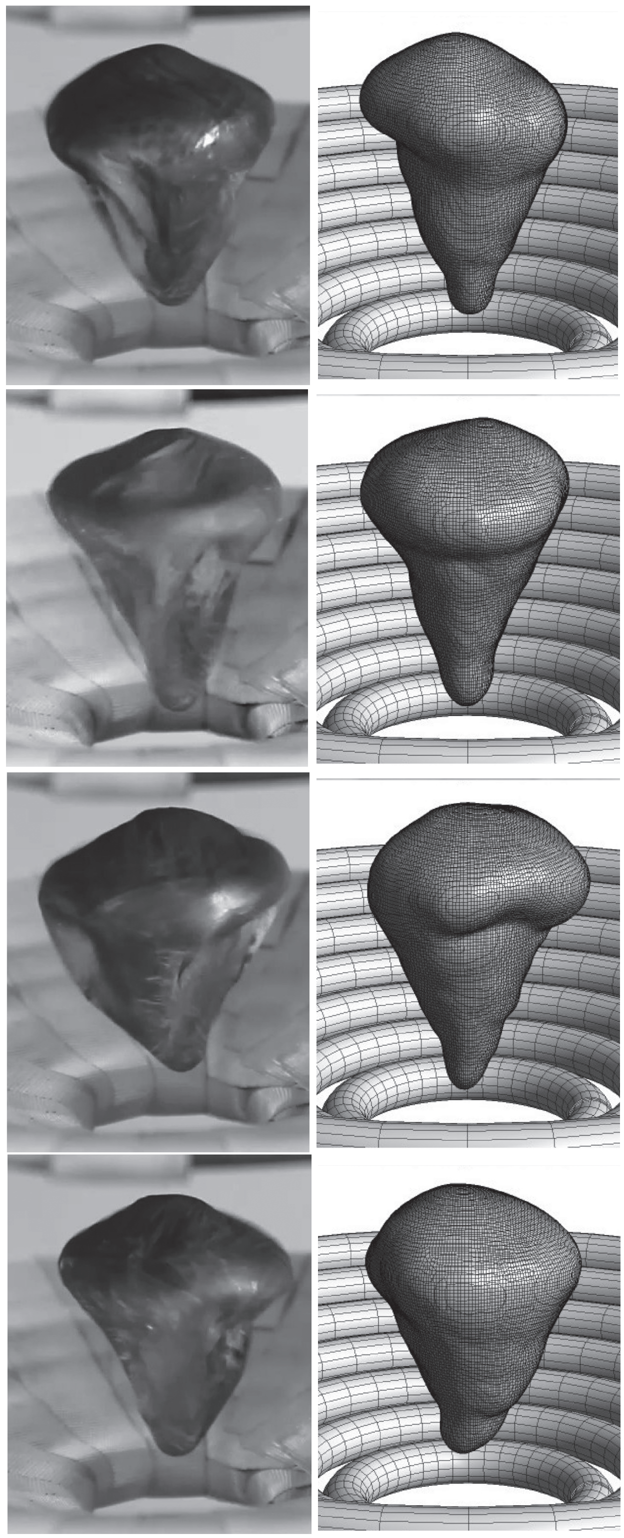

Fig. 2. Comparison of experimentally observed (top row) and 3D LES simulated (bottom row) instant free surface shape diversity.

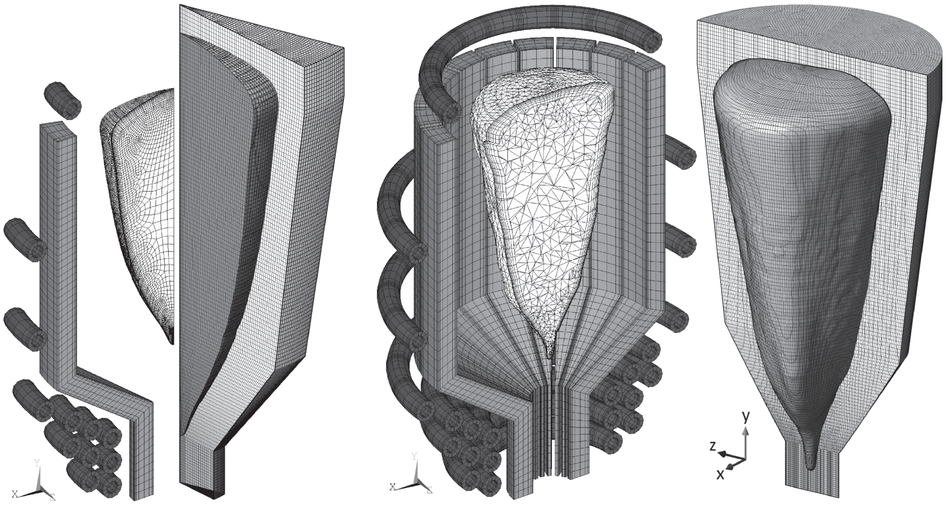

(*a*) (*b*)

Fig. 3. Numerical mesh for EM (on the left) and two-phase HD (on the right) calculation of molten titanium levitation used for a simplified model of a single CC section (*a*) and for a complete 3D model of the CC furnace and titanium charge (*b*).

In the HD part of the problem, k-ω SST and precise LES turbulence descriptions were used for the simulation of a single section and a full CC furnace, accordingly. Lorentz force f_{EM} recalculation upon the new free surface shape was performed every 6 ms of the flow time. The 3D LES simulation of 4.0 s of a fully developed flow took 1 month of the computation time on a cluster with 14 nodes (3 GHz each).

The following temperature independent material properties of liquid titanium were used: density $\rho_{\mathrm{Ti}} = 4110\,\mathrm{kg/m^3}$, surface tension $\gamma_{\mathrm{Ti}} = 1.557\,\mathrm{N/m}$, electrical conductivity $\sigma_{\mathrm{Ti}} = 0.56\,\mathrm{MS/m}$, and dynamic viscosity $\eta_{\mathrm{Ti}} = 4.42\,\mathrm{mPa{\cdot}s}$.

A modification of the cold crucible melting apparatus described in [9] was used for the numerical simulation of liquid titanium EM levitation. Our CC is composed of 20 palisades separated by gaps of 1.5 mm. The gap size can be increased, because no contact is expected between the CC and the levitated melt.

The bottom tapping nozzle has an inner diameter d_{noz} of 2 cm. This part of the CC is responsible for squeezing the EM field lines and increasing the field gradient in the critical null point region on the symmetry axis. A greater inner diameter d_{noz} will lead to a greater curvature radius of the melt at the bottom point and may cause a leakage; however, making d_{noz} too small makes it hard to install a cooling system in the palisades, as well as to drain the melt with no contact to the CC. The angle α between the cone-shaped bottom of the palisade and the horizontal xz-plane is $35°$.

Initially, the inner diameter of the CC walls d_{wall} was chosen to be 20 cm (Fig. 4*a*) in order to reduce the radial squeezing of the melt by EM forces. Radial EM pinching results in a greater height of the melt h and hydrostatic pressure p_h at the critical bottom point. However, in this case, the isosurface of the magnetic field inside the CC has a pronounced local maximum right above the nozzle. Because of that, the position and shape of the liquid metal is asymmetric, moreover, it might slide along this local ring-shaped EM field minimum from one palisade centre to another. The magnetic field distribution in the air inside the CC is shown below (Fig. 4*b*). In order to avoid this effect, d_{wall} was finally reduced to 10 cm.

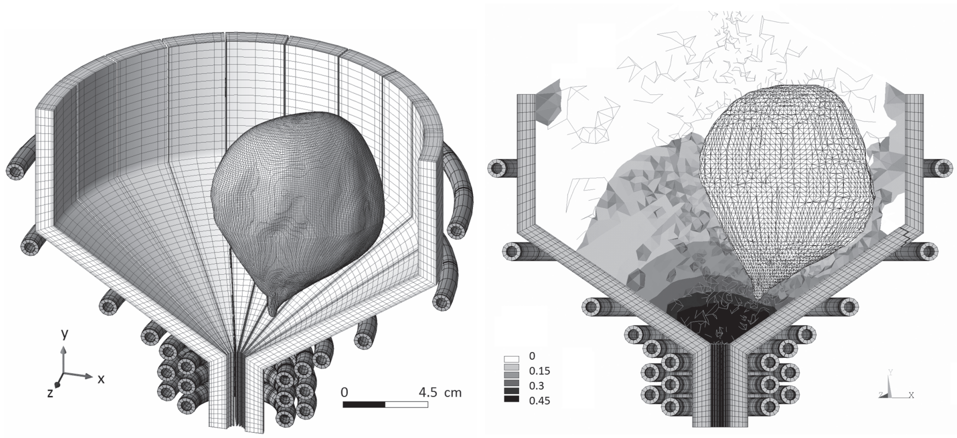

(a) (b)

Fig. 4. Asymmetric position of the levitated titanium (1 kg) in the CC furnace with $d_{\text{wall}} = 20$ cm obtained by 3D LES simulation (*a*) due to the expressed magnetic field maximum above the tapping nozzle (*b*).

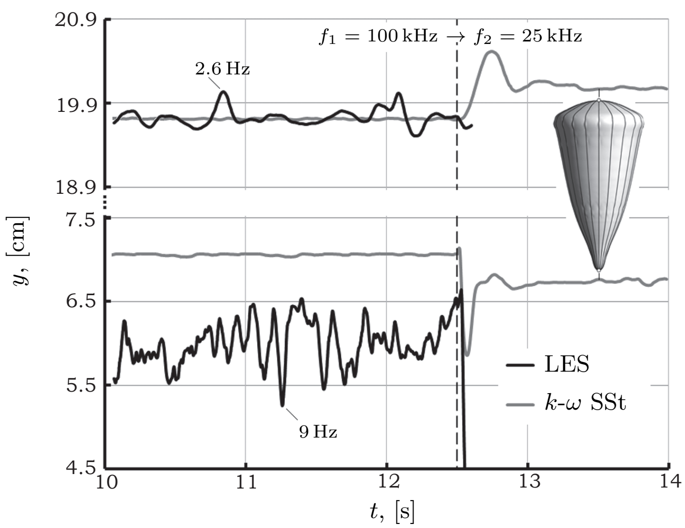

Fig. 5. Vertical oscillations of the molten titanium bottom and top free surface points on the symmetry axis of the setup obtained with the full 3D LES (black line) and simplified k-ω SST (grey line) models. The dashed line corresponds to an instant frequency switch from 100 kHz to 25 kHz.

11 turns of the inductor, mainly concentrated in the nozzle region, and an additional reverse turn above the crucible are fed with an effective current I_{eff} of 3.44 kA at a frequency f of 100 kHz.

4. Simulation results. Both numerical models predicted a successful levitation at the 100 kHz frequency, so it was decided to simulate the effect of the AC frequency switch from 100 kHz to 25 kHz on the levitated melt. For this purpose, a fully developed flow regime was simulated at 100 kHz and then the frequency was instantly reduced to 25 kHz and the current was slightly adjusted to ensure the same gravity compensating the y-component of the EM force.

The vertical oscillations of the molten titanium bottom and top free surface points (Fig. 5) indicate two different results: melt leakage in the case of 3D LES

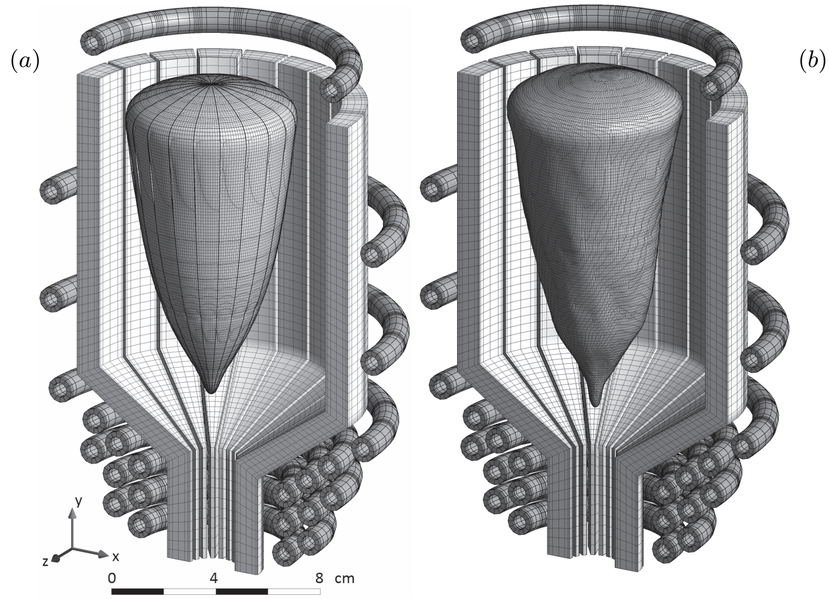

Fig. 6. Instant free surface shape of liquid titanium (1 kg) at 100 kHz obtained by the simplified k-ω SST calculation of a single section (a) and full 3D LES simulation of the CC levitation furnace (b).

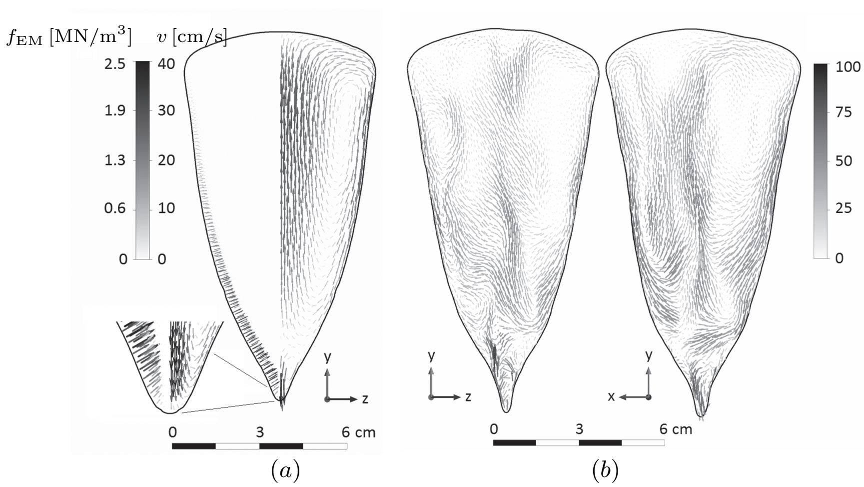

Fig. 7. The EM force (on the left) and the flow pattern (on the right) obtained by the k-ω SST calculation of a single section (a) and instant velocity pattern calculated with the full 3D LES model of the CC levitation furnace (b) at 100 kHz.

model and further levitation in the case of simplified k-ω SST calculation of a single section.

The free surface shape of liquid titanium for a fully developed flow regime at 100 kHz obtained by a simplified k-ω SST calculation of a single section and revolved for better visualization (Fig. 6a), as well as full 3D LES instant results of the CC levitation furnace (Fig. 6b) are shown.

According to the k-ω SST Reynolds-averaged calculation, the EM force, the free surface shape and the flow with a maximum velocity $v_{\max}$ of 40 cm/s adjust themselves to a nearly steady state regime with a big upper and a small lower vortex (Fig. 7a). Negligible free surface oscillations are hardly noticeable (Fig. 5).

Table 1. Summary of time-averaged simulation results obtained with the simplified k-ω SST calculation of a single CC section and 3D LES calculation of the whole CC furnace.

Numerical model	f, kHz	δ_{EM}, mm	$v_{\max}$, cm/s	h, cm	r_0, mm	p_h, kPa	p_γ, kPa	$(p_h$-$p_\gamma)/p_h$, %
Single section,	100	2.1	40	12.6	1.3	5.1	2.4	53
k-ω SST	25	4.3	57	13.4	2.8	5.4	1.1	80
Full 3D,	100	2.1	100	13.7	0.7	5.5	4.5	19
LES	25	4.3	–	–	–	–	–	–

The EM confinement clearly shows the lack of EM forces f_{EM} on the symmetry y-axis at the bottom of the melt, where the loop of the azimuthal eddy current has a zero radius (Fig. 7*a*).

Meanwhile, the finer flow structures resolved with LES reached up to 100 cm/s (Fig. 7*b*) and contributed to continuous free surface fluctuations, both noticeable in the lower and upper vortex region (Fig. 5). A Fourier transform shows that the upper free surface point on the symmetry y-axis of the setup oscillates with a frequency of 2.6 Hz, while the lower point oscillates with a higher frequency of 9 Hz.

Both models provided close results for the average free surface shape except for the lower part of the melt near the zero EM force region. The LES model predicts a more stretched bottom with the approximately twice less curvature radius r_0 at the bottom point of the melt, as well as a greater molten metal height h in contrast to the k-ω SST results (Table 1). The curvature radius r_0 at the

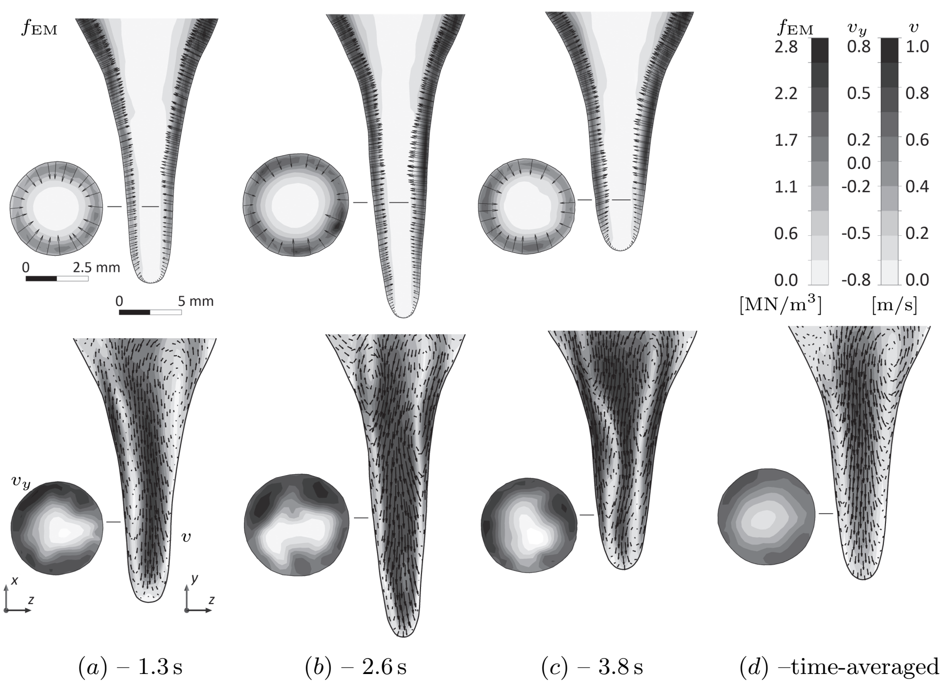

Fig. 8. The EM force (on the left) and the flow pattern (on the right) obtained by the k-ω SST calculation of a single section (*a*) and instant velocity pattern calculated with the full 3D LES model of the CC levitation furnace (*b*) at 100 kHz.

bottom point was calculated for the time-averaged shape by means of parabolic approximation.

Simple estimation of the surface tension pressure p_γ and hydrostatic pressure p_h in the zero EM force region at the bottom of the melt showed that for both models the surface tension was not enough to ensure the complete EM levitation at 100 kHz, however, no leakage was observed in our numerical calculations.

From the postprocessing of the 3D LES results it has appeared that the lowest point at the bottom of the melt is not simply moving along the symmetry y-axis. Because of the intensive turbulent flow it oscillates also in the xz-plane. The amplitude of these oscillations is 0.8 mm that gives 40% of the EM skin layer δ_{EM} of 2.1 mm at 100 kHz. Eventually, the time-averaged results prove that there is a minimum of the EM force at the bottom of the melt, however, it is not equal to zero and contributes to the pressure balance.

Two characteristic planes were chosen for the visualization of numerical results in the vicinity of critical confinement: the axial cross-section (yz-plane) and the horizontal slice parallel to the xz-plane at a fixed y-coordinate. The contours of the Lorentz force density, as well as the vectors at the free surface clearly illustrate the phenomenon of EM confinement at different time moments for the fully developed flow regime (Fig. 8). The lack of Lorentz forces at the bottom of the melt evidences of the main challenge of the CC levitation melting.

The contours of the y-velocity component v_y at the horizontal plane, as well as the velocity patterns on the axial cross-section indicate to the downward stream in the core flow and to the recirculation along the free surface of the melt (Fig. 8). Turbulent flow contributes to the oscillations of the bottom part of the levitated liquid metal.

The frequency switch from 100 to 25 kHz leads to an increase of the EM field penetration depth from 2.1 to 4.3 mm, for which the lower part of the melt with a small curvature radius of 0.7 mm becomes transparent. The initiated metal down-flow increases the curvature radius at the bottom and reduces the contribution of the surface tension, which results in the melt leakage predicted by our 3D LES calculation (Fig. 5).

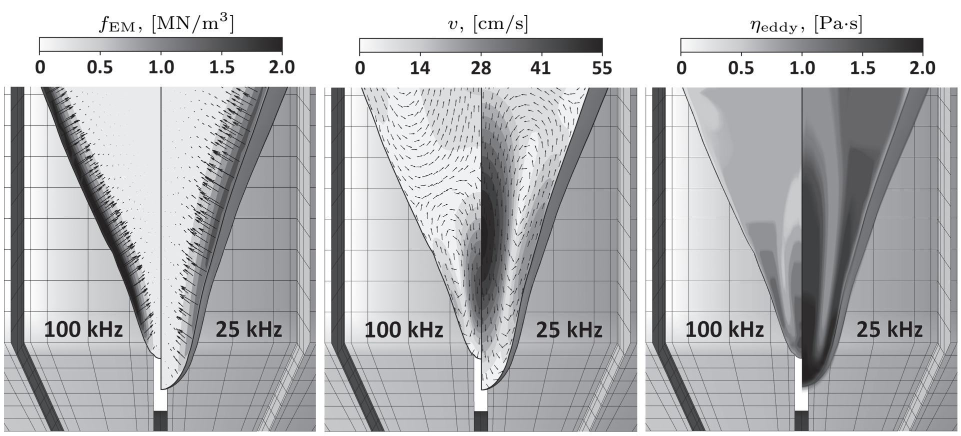

(a) (b) (c)

Fig. 9. Cross-sectional distribution of the Lorentz force density (a), velocity (b) and eddy viscosity (c) in the lower vortex region at a fully developed flow regime. Results are obtained with the simplified model of a single CC section with k-ω SST turbulence description for the AC frequency 100 kHz (on the left) and 25 kHz (on the right).

Meanwhile, in the simplified k-ω SST calculation of a single CC section, the movement of the bottom point of the melt was restricted by the symmetry y-axis. At the same time, the obtained curvature radius of 1.3 mm at the bottom point, where the EM force is always zero, is obviously not enough to satisfy the pressure balance and maintain the EM levitation at 100 kHz. The simulation results show that the k-ω SST turbulence model, especially combined with the VOF technique, predicts a very high eddy viscosity η_{eddy} in the lower vortex region. That is why the EM forces at some distance from the symmetry axis with account of prominent viscous stresses support the recirculated flow at the bottom. Moreover, the EM levitation is retained even after switching to the lower EM field frequency 25 kHz, when the curvature radius at the bottom increases up to 2.8 mm (Fig. 9).

We also observed the same overestimation of eddy viscosity by the k-ω SST model that made the conventional EM levitation [10] to be achieved in simulation with less efforts. 2D and 3D free surface flow models with the k-ω SST turbulence description predicted a stable EM levitation at lower inductor current and frequency values, while our 3D LES calculation and experiment gave evidences of the molten metal leakage already at the higher values of the current I_{eff} and frequency f [5], [11].

5. Conclusions.

• A numerical model for the calculation of liquid metal flow with free surface dynamics in the EM field has been developed and verified recently. Fine agreement with the experiment confirmed the enhanced accuracy of 3D LES calculation in contrast to the 2D and 3D k-ω SST simulation for the case of conventional EM levitation [11].

• Important design considerations of the CC levitation furnace have been obtained in the course of literature studies. Following this experience, a pilot design of the CC has been proposed and optimized by means of the numerical model in order to meet the conditions for the EM levitation of 1 kg of liquid titanium at 100 kHz.

• Simulation results show that finer flow structures resolved with LES reach up to 100 cm/s and contribute to continuous free surface fluctuations, while the k-ω SST calculation of a single section predicts a steady state free surface shape at a fully developed flow regime with a maximum velocity of 40 cm/s.

• Because of intensive turbulent flow and surface fluctuations precisely captured by the 3D LES model, the bottom of the levitated melt oscillates around the symmetry axis of the CC furnace. Therefore, the time-averaged results prove that there is a minimum of the EM force at the bottom of the melt, however, it is not equal to zero and compensates the 20% disbalance between the hydrostatic and surface tension pressure.

• In the case of k-ω SST calculation of a single section, the pressure disbalance at the bottom of the melt reaches 50% and cannot be compensated by the EM force, because the movement of the bottom point is restricted by the symmetry y-axis. The simulation results show that the k-ω SST turbulence model, combined with the VOF technique, overestimates the eddy viscosity that reaches more than 1 Pa·s in the lower vortex region and prominent viscous stresses prevent the recirculated flow from draining. Because of that, the EM levitation is retained even at the lower EM frequency 25 kHz, when the pressure disbalance at the bottom of the melt reaches 80% and the 3D LES model predicts the leakage.

• The higher EM frequency, in this case, contributes to the smaller radius at the bottom of the melt that increases the surface tension pressure term in the pressure balance and permits the EM confinement of greater liquid metal volumes.

• The 3D numerical calculation of the levitated liquid metal with free surface dynamics and induced turbulent flow resolved with the accurate LES turbulence model is in principle a new approach that permits a more precise and detailed investigation of free surface instabilities in levitation furnaces of different kinds. The developed approach will be used for the further investigation of levitation melting scale-up possibilities that meet industrial needs [12].

Acknowledgements. The current research was performed with the financial support of the ESF project of the University of Latvia, contract no. 2009/0138/1DP/1.1.2.1.2/09/IPIA/VIAA/004. The authors wish to thank the German Research Association for supporting this study under grant no. BA 3565/3-2.

REFERENCES

[1] M. Dumont, R. Ernst, C. Garnier, G. Hasan, P. Petitpas. Innovative inductive cold crucible configurations with improved efficiency. *Journal of Iron and Steel Research Int.*, vol. 19 (2012), no. 1, pp. 669–672.

[2] V. Bojarevics, A. Roy, K. Pericleous. Magnetic levitation of large liquid volume. *Magnetohydrodynamics*, vol. 46 (2010), no. 4, pp. 339–351.

[3] F.R. Block, A. Theissen. Das elektromagnetische Schwebeschmelzen - ein Beitrag zu den Verfahren des tiegelfreien Schmelzens. *Elektrowärme Int.*, vol. 29 (1971), no. 6, pp. 349–354 (in German).

[4] S. Spitans, A. Jakovics, E. Baake, B. Nacke. Numerical modelling of free surface dynamics of melt in an alternate EM field. Part I: implementation and verification of model. *Metallurgical and Materials Transactions B*, vol. 44 (2013), no. 3, pp. 593–605.

[5] S. Spitans, E. Baake, B. Nacke, A. Jakovičs. 3D LES two-phase simulation of conventional electromagnetic levitation experiment. In: *Proc. the 9th International Conference on Fundamental and Applied MHD, Thermoacoustic and Space Technologies,* (Riga, Latvia, 2014), vol. 2, pp. 261–265.

[6] S. Spitans, E. Baake, B. Nacke, A. Jakovics. New technology for electromagnetic levitation melting of metals. In: *Proc. the International Conference on Heating by Electromagnetic Sources* (Padua, Italy, 2013, addendum), pp. 1–8.

[7] H. Tadano, M. Fujita, T. Take, K. Nagamatsu, A. Fukuzawa. Levitation melting of several kilograms of metal with a cold crucible. *IEEE Transactions on Magnetics*, vol. 30 (1994), no. 6, pp. 4740–4742.

[8] G. Chintarin, G. Timelli, R. Losco, F. Bonollo. Development and operational experience on cold crucible levitation melting apparatus for light metal casting. In: *Proc. the International Conference on Heating by Electromagnetic Sources*, Padua, Italy, 2013, pp. 423–430.

[9] A. Morita, H. Fukui, H. Tadano, S. Hayashi, J. Hasegawa, M. Niinomi. Alloying titanium and tantalum by cold crucible levitation melting (CCLM) furnace. *Materials Science and Engineering*, vol. A280 (2000), pp. 208–213.

[10] E. Okress, D. Wroughton, G. Comenetz, P. Brace, J. Kelly. Electromagnetic levitation of solid and molten metals. *J. Applied Physics*, vol. 23 (1952), pp. 545–552.

[11] S. Spitans, E. Baake, B. Nacke, A. Jakovics. Numerical modelling of free surface dynamics of melt in an alternate EM field. Part II: conventional electromagnetic levitation. *Metallurgical and Materials Transactions B* (accepted 2015).

[12] S. Spitans, E. Baake, B. Nacke, A. Jakovičs. New technology for large scale electromagnetic levitation melting of metals. *Magnetohydrodynamics*, vol. 51 (2015), no. 1, pp. 121–132.

Received 13.02.2015